

# Theoretical analysis of optical mode deflection in lithium niobate waveguide with serrated array electrodes

Yuan Wang<sup>1,2</sup> · Zhe Chen<sup>1,2</sup> · Suxu Zhou<sup>1,2</sup> · Jianhui Yu<sup>1,2</sup> ·  
Yingxin Zeng<sup>1,2</sup> · Yunhan Luo<sup>1,2</sup> · Jun Zhang<sup>1,2</sup> ·  
Jieyuan Tang<sup>1,2</sup> · Heyuan Guan<sup>1,2</sup> · Huihui Lu<sup>1,2</sup>

Received: 2 October 2015 / Accepted: 22 January 2016 / Published online: 3 February 2016  
© Springer Science+Business Media New York 2016

**Abstract** In this paper, we establish a lithium niobate (LN) thin film planar waveguide and an annealed proton exchange (APE) waveguide model with serrated array electrodes configuration to deflect and reshape the optical mode. The refractive index profile of the waveguide can be electro-optically manipulated by applying an external voltage into the serrated array electrodes. Through the simulation results, it is observed that different refractive index manipulation of LN waveguide can make the optical beam have different deflection and reshaping. The comparison between the thin film and APE bulk planar waveguide is investigated. When the beam deflection is modulated via the high-speed electro-optic effect of LN, the temporal and spatial beam smoothing can be achieved for the application of high power laser system and other optical signal processing.

**Keywords** Lithium niobate waveguide · Serrated array electrodes · Mode deflection

---

This article is part of the Topical Collection on Numerical Simulation of Optoelectronic Devices, NUSOD' 15.

---

Guest Edited by Julien Javaloyes, Weida Hu, Slawek Sujecki and Yuh-Renn Wu.

---

✉ Huihui Lu  
thuihuilu@jnu.edu.cn  
  
Jianhui Yu  
kensomyu@gmail.com

<sup>1</sup> Key Laboratory of Optoelectronic Information and Sensing Technologies of Guangdong Higher Educational Institutes, Jinan University, Guangzhou 510632, China

<sup>2</sup> Department of Optoelectronic Engineering, Jinan University, Guangzhou 510632, China

## 1 Introduction

One of the vital requirements in ultrahigh power laser drivers is beam smoothing in the target surface. The optical beam smoothing technology can be divided into spatial and temporal smoothing technologies (Deng et al. 2013). The spatial smoothing technologies include continuous phase plates (CPP) (Lin et al. 1996), distributed phase plates (DPP) (Lin et al. 1995), random phase plates (RPP) (Kato et al. 1984) and lens arrays (LA) technique (Deng et al. 1986). While the temporal smoothing technologies include inducing spatial incoherence (ISI) (Lehmberg et al. 1987), smoothing by spectral dispersion (SSD) (Skupsky et al. 1989), etc. Nowadays, the widely utilized technology is smoothing by spectral dispersion (SSD). The light source is a relatively broadband light which is produced by electro-optic phase modulation and dispersed by grating (Skupsky et al. 1989). If the light beam dithers in a small range, light spot will quickly move in the focal plane. Therefore, it produces optical mode deflection and a beam smoothing effect in the average time through the high-speed electro-optic phase modulation. However, when a broadband light source is produced by sinusoidal frequency-modulation, the beam smoothing effect of SSD is not obvious (Zhou et al. 2007).

Various methods and proposals have been suggested for mode deflection to achieve beam smoothing, the optical waveguides were proposed in previous reports, such as using a Ti-diffusion LN waveguide with acousto-optic Bragg deflection (Schmidt and Kaminow 1975), acousto-optic deflection in  $\text{Ta}_2\text{O}_5$  waveguides (Douglas and Michael 1974), electro-optic beam deflection using the leaky mode of a planar waveguide (Himel et al. 1991), liquid crystal optical phased array (Pan et al. 2012), planar waveguides via grating rotation (Veith et al. 1995), solid-state ultrafast all-optical streak camera in a GaAs/AlGaAs planar waveguide (Sarantos and Heebner 2010) and chip scale GaAs device with Mach–Zehnder Interferometer (Shih et al. 2012). These waveguide configurations were employed for many specific applications, but either the high-speed modulation cannot be reached, or require powerful driving voltage. Recent years, micro and nanostructured waveguide were introduced for deflecting the guided mode. The superprism effect in lithium niobate photonic crystals was fabricated for ultra-fast, ultra-compact electro-optical switching (Amet et al. 2008; Lu et al. 2014), nanoscale plasmonic devices (Çetin et al. 2010) and unidirectional fishnet metamaterials (Rodríguez-Ulibarri et al. 2015) were also proposed, these configurations can probably reduce the driving energy, but complicated micro and nanostructure should be fabricated which induce the loss and lead to intricate fabrication process.

LN is one of most extensively used materials in optical communication, and is a versatile optical candidate material since it possesses excellent electro-optic, acousto-optic, piezoelectric, and nonlinear properties (Lu et al. 2013). Moreover, it has a large transparency range (0.4–5  $\mu\text{m}$ ) and a wide intrinsic bandwidth. The most popular approaches to fabricate the LN optical waveguide are annealed proton exchange (APE) and ion doped method such as titanium in-diffusion (Wooten et al. 2000; Lu et al. 2012), which can fabricate the LN waveguide with very low propagation loss.

In this paper, an optical planar waveguide and an annealed proton exchange (APE) waveguide model with serrated array electrodes configuration are proposed for beam deflection. Through the electro-optic effect of LN, the distribution of refractive index in waveguide with serrated array electrodes can slightly be manipulated, which creates the refractive index prism array to deflect the optical mode. The configurations are quite simple and do not require the complicated micro and nanostructure. Moreover, it is

compatible with the optical waveguide made of electro-optic material, and it can potentially achieve the beam smoothing with a relatively low driving voltage. The high-speed electro-optic modulation makes the intensity profile of output mode modulated with a high speed, so the light beam will be deflected and reshaped through the electro-optic effect of LN waveguide.

## 2 Conventional APE waveguide and results

The 7  $\mu\text{m}$  wide LN straight waveguide model has been proposed in our previous report (Wang et al. 2014), as shown in Fig. 1, which can obtain slightly mode deflection via the electro-optic tuning through experimental results, it reveals that the horizontal mode deflection was not evident when different voltages applied as shown in Fig. 2. Therefore, novel theoretical models are proposed to demonstrate and improve the deflection and reshaping of optical mode.

## 3 LN thin film planar waveguide

Figure 3 is a Z-cut LN thin film planar waveguide with metal electrode (NANOLN:<http://www.nanoln.com/product/lnoi-with-metal-electrode-ii>). The thickness of the LN thin film is  $\sim 0.6 \mu\text{m}$ . A metal electrode layer (Au) between the  $\text{SiO}_2$  layer (optical insulation layer) and the LN substrate is inserted by deposition. Electric field can be applied on the LN thin film between this metal electrode layer and a top electrode layer.

The simulated model is composed by a LN thin film planar waveguide with serrated array electrodes, which is displayed as Fig. 4. The operating wavelength ( $\lambda$ ) is of 1.064  $\mu\text{m}$ , the width of the planar waveguide is 50  $\mu\text{m}$ , the thickness and the refractive index of LN substrate are 500  $\mu\text{m}$  and 2.156 respectively, the electrode layer between  $\text{SiO}_2$  layer and LN substrate is deposited as ground with thickness of 0.2  $\mu\text{m}$ , the thickness and the refractive index of  $\text{SiO}_2$  layer are 1  $\mu\text{m}$  and 1.40 respectively. Serrated array electrodes with 25 periods are imprinted on the top of LN thin film, the lateral extend of serrated array is 50  $\mu\text{m}$ , and the longitudinal pitch of a serrated pattern is 60  $\mu\text{m}$ . An external voltage can be applied on the LN thin film between the ground electrode layer and the top electrode layer, which produces electric field distribution in the waveguide as shown in Fig. 5.

The refractive index profile in LN waveguide can be changed through the electro-optic effect by applying different voltages to the serrated array electrodes, the electric field distribution calculation was performed by using finite element method (Comsol), the

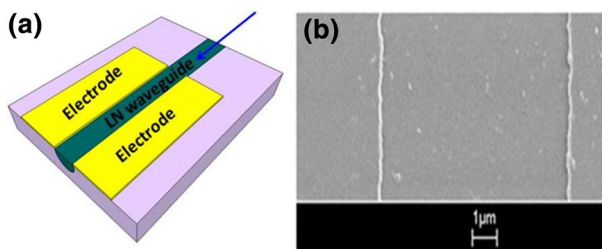


**Fig. 1** a Straight waveguide model and b its fabricated SEM image

**Fig. 2** Experimental result of cross-sectional optical mode deflection in horizontal direction

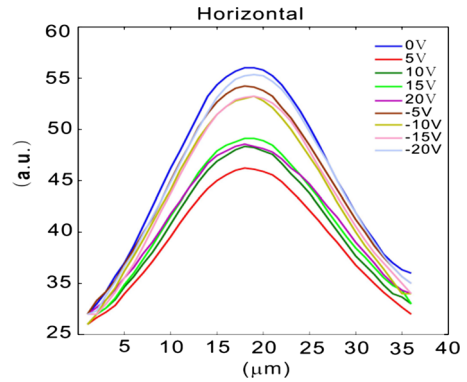


**Fig. 3** LN thin film planar waveguide with metal electrode layer

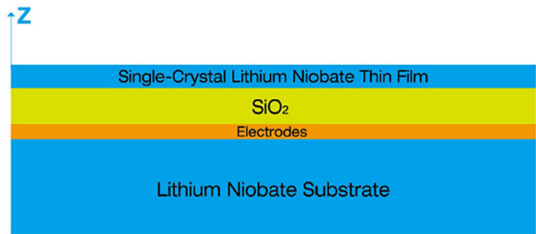
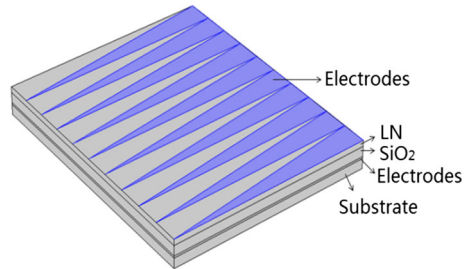


**Fig. 4** LN thin film planar waveguide configured with serrated array electrodes



refractive index distribution of the waveguide acts as prism array to deflect the optical mode, and it makes different optical mode profiles in the end-fire of planar waveguide corresponding to the different applied voltages. The equations were solved with Comsol as follows:

$$\mathbf{E} = -\nabla V$$

$$\nabla \cdot (\epsilon \mathbf{E}) = \rho_v$$

where,  $\mathbf{E}$  is electric field,  $V$  is electric potential,  $\epsilon$  is permittivity, and  $\rho_v$  is charge density. Through the above equations, the electric field distribution  $\mathbf{E}(x, y, z)$  can be obtained as displayed in Fig. 5.

The ordinary refractive index  $n_o$  can be neglected in electro-optic effect (Chen 1969). If we apply an external voltage on LN induced the spatially electric field distribution, its index of refraction changes ( $\Delta n_e$ ) according to the Pockels equation as follows:

**(a)** Time=1 Slice:Electric field norm (V/m) **(b)** Time=1 Slice:Electric field norm (V/m)

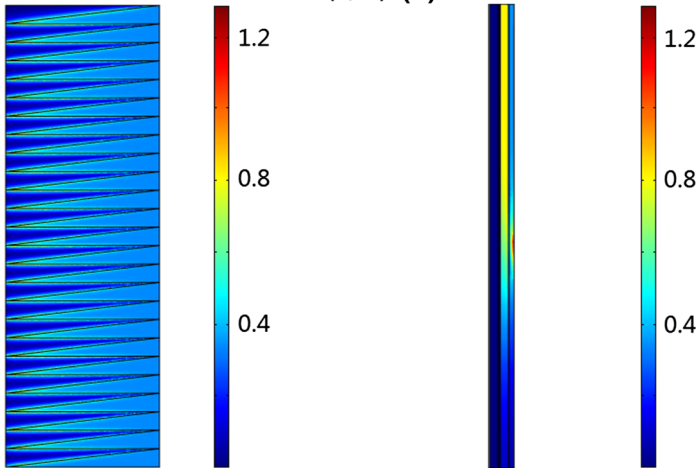


**Fig. 5** Electric field distribution in LN thin film planar waveguide **a** Horizontal top view; **b** Sectional view

$$\Delta n(x, y, z) = -\frac{n_e^3 \gamma_{33} E(x, y, z)}{2}$$

where,  $\gamma_{33}$  is electro-optical coefficient,  $n_e$  is extraordinary refractive index,  $E$  is the electric field which was calculated previously in Fig. 5 yielding the electric field distribution  $E(x, y, z)$ .

The beam propagation method (Rsoft) is employed to calculate the optical mode propagating in the LN thin film planar waveguide with different applied voltages corresponding different electric field distribution. The obtained refractive index profile  $n(x, y, z) = n_e + \Delta n(x, y, z)$  can be included in BPM resolved equation. The basic BPM equation in three dimensions is as follows:

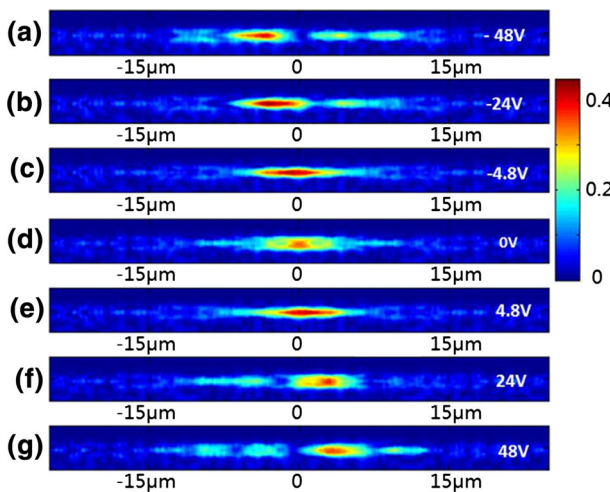


**Fig. 6** Optical mode profile in output of 50  $\mu\text{m}$  wide LN thin film planar waveguide when applied voltages are: **a** -48 V; **b** -24 V; **c** -4.8 V; **d** 0 V (no applied voltage); **e** 4.8 V; **f** 24 V; **g** 48 V

$$\frac{\partial u}{\partial z} = \frac{i}{2k} \left( \frac{\partial^2 u}{\partial x^2} + \frac{\partial^2 u}{\partial y^2} + (k^2 - \bar{k}^2)u \right)$$

where,  $u$  is the slowly varying field,  $k$  is the spatially dependent wavenumber, via  $k = k_0 n(x, y, z)$ ,  $\bar{k}$  is the reference wavenumber to be chosen to represent the average phase variation of the field, via  $\bar{k} = k_0 \bar{n}$ .

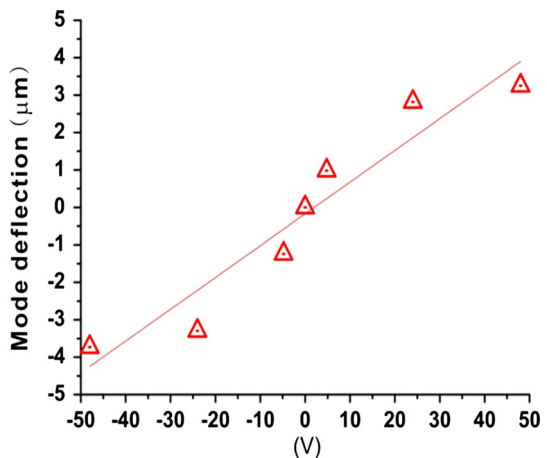
The size of incident Gaussian mode is of  $4 \mu\text{m} \times 0.6 \mu\text{m}$ , and the beam waist is  $\sim 3 \mu\text{m}$ . The output of optical mode profile is monitored in the end-fire of waveguide, which can analyze the mode deflection. Figure 6d represents the optical mode profile of LN thin film planar waveguide before applying a voltage to the serrated array electrodes (0 V). Figure 6a–c, e–g represent the optical mode profiles in the end-fire of waveguide when applied voltages are  $-48$ ,  $-24$ ,  $-4.8$ ,  $4.8$ ,  $24$  and  $48$  V respectively. The difference between them is that different refractive index profiles of LN waveguide bellow serrated array electrodes can be realized. Figure 7 shows the relationship between the mode deflection and different applied voltages in  $50 \mu\text{m}$  wide LN thin film planar waveguide, which concludes the mode deflection in the horizontal direction.

According to the simulation results, the different refractive index manipulation of LN planar waveguide can make the optical beam have different mode deflection. Since in  $50 \mu\text{m}$  wide LN thin film planar waveguide configuration, the distance of electrodes is  $< 2 \mu\text{m}$ , the electro-optic effect of LN waveguide is more intensive and sensible, with a driving voltage of  $4.8$  V, the mode deflection can achieve  $\sim 1 \mu\text{m}$ . Therefore, this decreases the driving voltage of mode deflection. The higher applied voltage can obtain an enhanced contrast refractive index prism array, which leads to larger mode deflection.

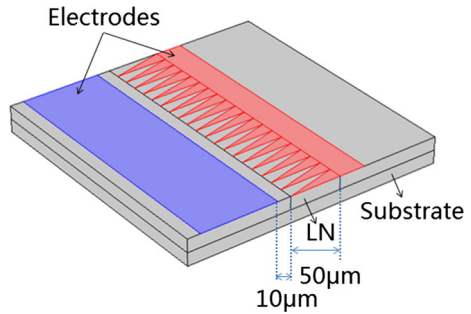
#### 4 APE planar waveguide

Figure 8 is a  $50 \mu\text{m}$  wide APE waveguide with coplanar serrated array electrodes. The operating wavelength ( $\lambda$ ) is of  $1.064 \mu\text{m}$ , and the refractive index of LN waveguide and the substrate are 2.161 (due to APE process) and 2.156 respectively, the thickness of the waveguide and substrate are  $\sim 2.5$  and  $500 \mu\text{m}$  respectively, the top electrode layer includes the blue area which is set as ground and the red area as anode, a metal (Au)

**Fig. 7** Mode deflection as a function of different applied voltages in  $50 \mu\text{m}$  wide LN thin film planar waveguide



**Fig. 8** APE waveguide with coplanar serrated array electrodes



serrated array with 25 periods is imprinted in the red area, the lateral extend of serrated array is  $50\ \mu\text{m}$  (equals to the width of APE waveguide), and the longitudinal pitch of a serrated pattern is  $60\ \mu\text{m}$ . The distance between the ground electrode and the top of triangular serrated array electrodes is of  $10\ \mu\text{m}$  as illustrated in Fig. 8.

Electric field can be applied on the LN waveguide between the ground and the anode, as shown in Fig. 9. The size of incident Gaussian mode is of  $8\ \mu\text{m} \times 2.5\ \mu\text{m}$ , and the beam waist is  $\sim 6\ \mu\text{m}$ . With applying different voltages to the electrodes, it can make different optical mode profiles in output of waveguide as Fig. 10. Figure 10d represents the optical mode profile before applying a voltage to the serrated array electrodes. Figure 10a–c, e–g represent the optical mode profile when the electrodes were applied  $-125$ ,  $-75$ ,  $-25$ ,  $25$ ,  $75$  and  $125\ \text{V}$  respectively, and the relationship between the mode deflection and refractive index changes in  $50\ \mu\text{m}$  wide LN APE waveguide is depicted in Fig. 11.

The APE waveguide with serrated array electrodes can also deflect the optical guided multi-modes; even it requires higher applied voltage as its electrodes are widely spaced comparing to the LN thin film planar waveguide. According to the simulation results, with  $25\ \text{V}$  applied to the electrodes,  $\sim 2\ \mu\text{m}$  mode deflection can be realized. Due to the refractive index contrast between APE LN and LN substrate is lower than that of LN thin film planar waveguide configuration, the optical mode is not so confined in the APE waveguide. Since the electrodes of APE waveguide can be deposited in coplanar structure, the design is more flexible for fabrication.

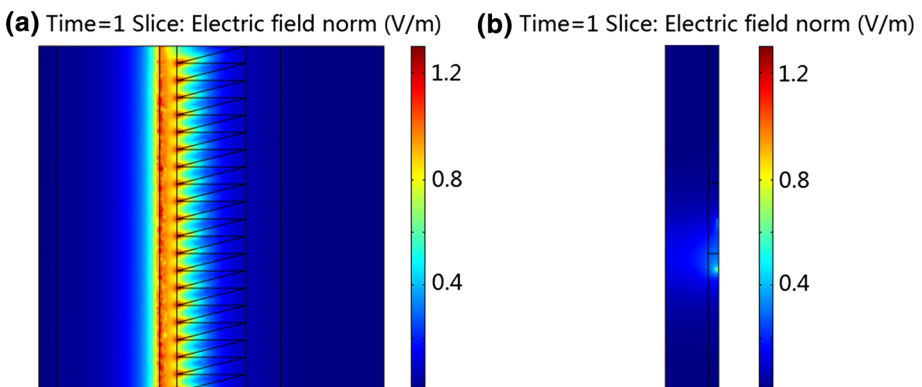


**Fig. 9** Electric field distribution in  $50\ \mu\text{m}$  wide APE waveguide: **a** Horizontal top view; **b** Sectional view

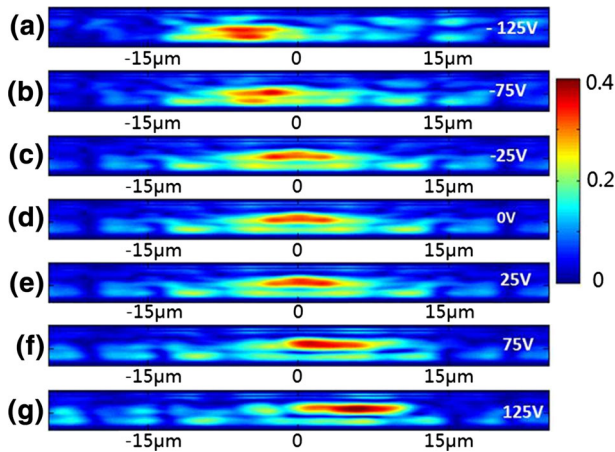
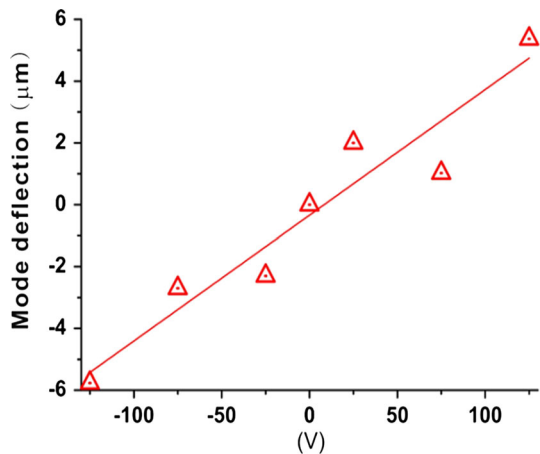


**Fig. 10** Optical mode profile in output of 50  $\mu\text{m}$  wide APE waveguide when applied voltages are: **a**  $-125\text{ V}$ ; **b**  $75\text{ V}$ ; **c**  $-25\text{ V}$ ; **d**  $0\text{ V}$  (no applied voltage); **e**  $25\text{ V}$ ; **f**  $75\text{ V}$ ; **g**  $125\text{ V}$

**Fig. 11** Mode deflection as a function of different applied voltages in 50  $\mu\text{m}$  wide APE waveguide



## 5 Conclusion

In summarize, through the simulated results, we observe that the different refractive index manipulation of LN waveguide with serrated array electrodes configuration can make the optical beam have different deflection and reshaping. The beam deflection scale depends on the difference of refractive index distribution which can be manipulated through the electro-optic effect via external applied voltages. The comparison of thin film and APE planar waveguide indicates that the thin film planar can reduce the applied voltage thanks to its compact electrodes which is not as long spaced as the APE waveguide structure. This performance can be potentially utilized for mode deflection in high speed regime, moreover, it can be exploited to the beam smoothing for the application of high power laser system and other optical signal processing.



**Acknowledgments** This work was supported by Jinan University's Scientific Research Creativeness Cultivation Project for Outstanding Undergraduates Recommended for Postgraduate Study, the National Natural Science Foundation of China (No. 61405075; No. 61177075; No. 61275046; No. 61475066; No. 61505069; No. 61575084), Special Funds for Discipline Construction of Guangdong Province (2013CXZDA005), Natural Science Foundation of Guangdong Province (No. 2015A030306046; No. 2014A030313377, No. 2015A030313320), Special Funds for major science and technology projects of Guangdong Province (2014B010120002, 2014B010117002, 2015B010125007), Planned Science and Technology Project of Guangzhou under Grant (201506010046), Young and Innovative Talents Project of Guangdong High Education (2014KQNCX025).

## References

- Amet, J., Baida, F.I., Burr, G.W., et al.: The superprism effect in lithium niobate photonic crystals for ultrafast, ultra-compact electro-optical switching. *Photonics Nanostruct. Fundam. Appl.* **6**, 47–59 (2008)
- Çetin, A.E., Sennaroglu, A., Müstecaplıoğlu, Ö.E., et al.: Nanoscale plasmonic devices for dynamically controllable beam focusing and scanning. *Photonics Nanostruct. Fundam. Appl.* **8**, 7–13 (2010)
- Chen, F.S.: Optically induced change of refractive indices in  $\text{LiNbO}_3$  and  $\text{LiTaO}_3$ . *J. Appl. Phys.* **40**, 3389–3396 (1969)
- Deng, X., Liang, X., Chen, Z., et al.: Uniform illumination of large targets using a lens array. *Appl. Opt.* **25**, 377–381 (1986)
- Deng, J., Xiquan, F., Zhang, L., et al.: Fresnel diffraction and small-scale self-focusing of a phase modulated and spectrally dispersed laser beam. *Opt. Laser Technol.* **45**, 56–61 (2013)
- Douglas, A.W., Michael, C.H.: Acousto-optic deflection in  $\text{Ta}_2\text{O}_5$  waveguides. *Appl. Phys. Lett.* **24**, 159–161 (1974)
- Himel, M.D., Shi, X., Hu, X.Q., et al.: Electrooptic beam deflection using the leaky mode of a planar waveguide. *IEEE Photonics Technol. Lett.* **3**, 921–923 (1991)
- Kato, Y., Mima, K., Miyanaga, N., et al.: Distributed phase plates for super-Gaussian focal-plane irradiance profiles. *Phys. Rev. Lett.* **53**, 1057–1060 (1984)
- Lehmberg, R.H., Schmitt, A.J., Bodner, S.E.: Theory of induced spatial incoherence. *J. Appl. Phys.* **62**, 2680–2701 (1987)
- Lin, Y., Kessler, T.J., Lawrence, G.N.: Distributed phase plates for super-Gaussian focal-plane irradiance profiles. *Opt. Lett.* **20**, 764–766 (1995)
- Lin, Y., Kessler, T.J., Lawrence, G.N.: Design of continuous surface-relief phase plates by surface-based simulated annealing to achieve control of focal-plane irradiance. *Opt. Lett.* **21**, 1703–1705 (1996)
- Lu, H., Baida, F.I., Ulliac, G., et al.: Lithium niobate photonic crystal wire cavity: realization of a compact electro-optically tunable filter. *Appl. Phys. Lett.* **101**, 151117–151120 (2012)
- Lu, H., Sadani, B., Ulliac, G., et al.: Integrated temperature sensor based on an enhanced pyroelectric photonic crystal. *Opt. Express* **21**, 16311–16318 (2013)
- Lu, H., Qiu, W., Guyot, C., et al.: Optical and RF characterization of a lithium niobate photonic crystal modulator. *IEEE Photonics Technol. Lett.* **26**, 1332–1335 (2014)
- NANOLN. <http://www.nanoln.com/product/loi-with-metal-electrode-ii>
- Pan, F., Kong, L., Yang, X., et al.: Dual beam deflection of liquid crystal optical phased array. *Chin. Opt. Lett.* **10**, S20502.1–S20502.5 (2012)
- Rodríguez-Ulibarri, P., Pacheco-Peña, V., Navarrocía, M., et al.: Experimental demonstration of deflection angle tuning in unidirectional fishnet metamaterials at millimeter-waves. *Appl. Phys. Lett.* **106**, 061109–061113 (2015)
- Sarantos, C.H., Heebner, J.E.: Solid-state ultrafast all-optical streak camera enabling high-dynamic-range picosecond recording. *Opt. Lett.* **35**, 1389–1391 (2010)
- Schmidt, R.V., Kaminow, I.P.: Acoustooptic Bragg deflection in  $\text{LiNbO}_3$  Ti-diffused waveguides. *IEEE J. Quantum Electron.* **11**, 57–59 (1975)
- Shih, T.-M., Sarantos, C., Haynes, S.M., et al.: Chipscale, single-shot gated ultrafast optical recorder. *Opt. Express* **20**, 414–425 (2012)
- Skupsky, S., Short, R.W., Kessler, T., et al.: Improved laser-beam uniformity using the angular dispersion of frequency-modulated light. *J. Appl. Phys.* **66**, 3456–3462 (1989)
- Veith, M., Müller, K.G., Mittler-Neher, S., et al.: Propagation and deflection of guided modes in planar waveguides via grating rotation. *Appl. Phys. B* **60**, 1–4 (1995)

- Wang Y et al. Numerical simulation of optoelectronic devices (NUSOD), 2014 14th International Conference on. IEEE, pp 75–76, (2014) NANOLN:<http://www.nanoln.com/product/Inoi-with-metal-electrode-ii>
- Wooten, E.L., Kissa, K.M., Yi-Yan, A., et al.: A review of lithium niobate modulators for fiber-optic communications systems. Selected Top. Quantum Electron. IEEE J. **6**, 69–82 (2000)
- Zhou, S., Lin, Z., Jiang, X.: Beam smoothing by lens array with spectral dispersion. Opt. Commun. **272**, 186–191 (2007)